Cyclophanes

DOI: 10.1002/anie.201403816

Electron Delocalization in a Rigid Cofacial Naphthalene-1,8:4,5-bis(dicarboximide) Dimer**

Yilei Wu, Marco Frasconi, Daniel M. Gardner, Paul R. McGonigal, Severin T. Schneebeli, Michael R. Wasielewski, and J. Fraser Stoddart**

Abstract: *Investigating through-space electronic communication between discrete cofacially oriented aromatic π-systems is fundamental to understanding assemblies as diverse as double-stranded DNA, organic photovoltaics and thin-film transistors. A detailed understanding of the electronic interactions involved rests on making the appropriate molecular compounds with rigid covalent scaffolds and π–π distances in the range of ca. 3.5 Å. Reported herein is an enantiomeric pair of doubly-bridged naphthalene-1,8:4,5-bis(dicarboximide) (NDI) cyclophanes and the characterization of four of their electronic states, namely 1) the ground state, 2) the exciton coupled singlet excited state, 3) the radical anion with strong through-space interactions between the redox-active NDI molecules, and 4) the diamagnetic diradical dianion using UV/Vis/NIR, EPR and ENDOR spectroscopies in addition to X-ray crystallography. Despite the unfavorable Coulombic repulsion, the singlet diradical dianion dimer of NDI shows a more pronounced intramolecular π–π stacking interaction when compared with its neutral analog.*

Aromatic stacking is ubiquitous in biological systems, where it plays significant roles, for example, in defining molecular recognition sites[1] in double-stranded DNA and in enabling excitonic coupling[2] in photosynthetic systems. In synthetic materials, such as those used in organic electronic devices,[3] π-electron delocalization between molecules along aromatic stacks is responsible[4] for electrical conductivity. An understanding of the electronic interactions, which couple cofacially stacked redox-active π-systems, is therefore desirable for charge transport optimization in organic electronic and magnetic materials. The efficiency of intermolecular charge transport in organic semiconductors is governed[4] by 1) electronic coupling, which depends on the overlap of molecular orbitals between neighboring molecules, and 2) the total reorganization energy for charge transport between redox centers. Both of these factors are closely linked to the relative orientations and intermolecular distances of the molecules in the solid state, i.e., the way in which the molecules pack together.[5] Although the exact structure–performance correlation is still not well understood, considerable efforts[6] are currently being devoted towards reaching this goal. In general, the close packing of molecules with significant intramolecular π-orbital overlap allows for enhanced charge transport properties.[7] The ability to assemble well-defined stacks is expected to lead to the development of advanced organic materials with unprecedented performance.[8] Since the parallel cofacial organization of aromatic units in register is not always energetically favorable,[9] the synthesis of discrete face-to-face aromatic stacks poses a challenge. In order to confront this challenge, we have designed and synthesized a discrete covalently linked naphthalene-1,8:4,5-bis(dicarboximide) (NDI) dimer (Figure 1a) and investigated the electronic interactions between its two π-aromatic faces.

NDI derivatives[10] are a class of electron-deficient aromatic compounds capable, inter alia, of self-assembly,[11] charge transport,[12] chemosensing,[13] synthetic membrane-transport,[14] and selective catalysis.[15] Their versatility has resulted in their extensive use in the construction of mechanically interlocked molecules[16] with potential applications in organic electronic devices. These diimides are neutral, planar, chemically robust, and exhibit a rich redox chemistry. Although examples of covalently attached NDI dimers have been reported previously,[17–18] their lack of rigidity[17] and large interplanar distances[18] of >4.5 Å have thus far precluded their use as electron transfer mediators in close-to-ideal aromatic stacks. Herein, we describe an enan-

[*] Y. Wu, Dr. M. Frasconi, Dr. P. R. McGonigal, Dr. S. T. Schneebeli, Prof. J. F. Stoddart
Center for the Chemistry of Integrated Systems
Department of Chemistry, Northwestern University
2145 Sheridan Road, Evanston, IL 60208-3113 (USA)
E-mail: stoddart@northwestern.edu
Y. Wu, D. M. Gardner, Prof. M. R. Wasielewski
Argonne-Northwestern Solar Energy Research (ANSER) Center,
Department of Chemistry, Northwestern University
2145 Sheridan Road, Evanston, IL 60208-3113 (USA)
E-mail: m-wasielewski@northwestern.edu

[**] We thank Dr. Saman Shafaie for collecting high-resolution mass spectrometric data, Dr. Charlotte L. Stern and Dr. Amy A. Sarjeant for solving the single-crystal X-ray structures, and Rufei Shi for helpful discussions. This research is part (Project 32-949) of the Joint Center of Excellence in Integrated Nano-Systems (JCIN) at King Abdul-Aziz City for Science and Technology (KACST) and Northwestern University (NU). The authors would like to thank both KACST and NU for their continued support of this research. M.R.W. was supported by the Chemical Sciences, Geosciences, and Biosciences Division, Office of Basic Energy, DOE, under grant no. DEFG02-99ER-14999. S.T.S. thanks the International Institute for Nanotechnology (IIN) at NU for an IIN Postdoctoral Fellowship and the QUEST high-performance computing center at NU for a research allocation of computer time. P.R.M. acknowledges support from the National Science Foundation (NSF) (CHE-1308107) and thanks the US-UK Fulbright Commission for an All-Disciplines Scholar Award. Y.W. thanks the Fulbright Scholars Program for a Graduate Research Fellowship.

Supporting information for this article is available on the WWW under http://dx.doi.org/10.1002/anie.201403816.

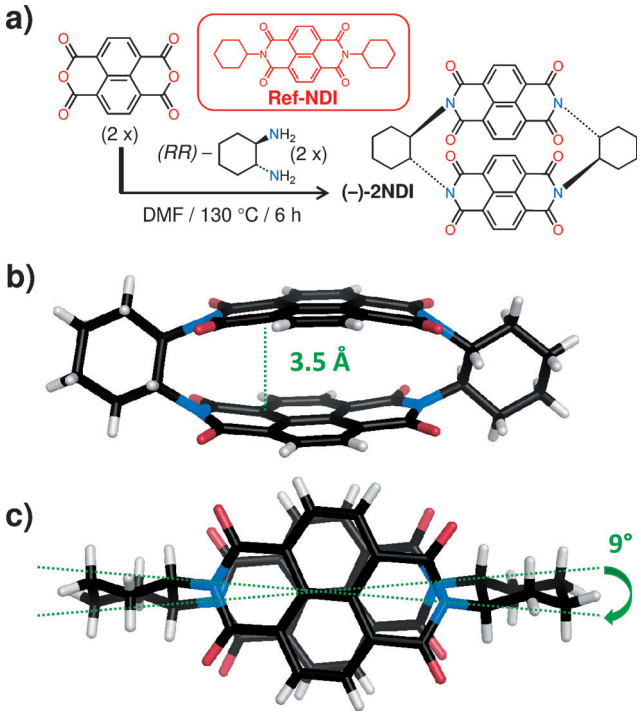

Figure 1. a) Stereospecific synthesis of the rigid cyclophane dimer (−)-**2NDI** from (*RR*)-*trans*-1,2-cyclohexanediamine and naphthalenetetracarboxylic dianhydride. The enantiomer (+)-**2NDI** was obtained in a similar fashion from (*SS*)-*trans*-1,2-cyclohexanediamine. Tubular representations of the b) plan, and c) side-on views of solid-state structures of (−)-**2NDI**, showing the close intramolecular distance and twist angle between the two NDI units.

tiomeric pair of chiral cyclophanes, (−)- and (+)-**2NDI**, each containing two cofacially assembled NDI units, held rigidly at a π–π distance (Figure 1b) of 3.5 Å, similar to the interlayer distance in graphite.[19] This enforced aromatic stacking brings about several emergent redox and photophysical properties that are not observed either in solution or in the solid state for their monomeric analog **Ref-NDI**. In solution, strong intramolecular electronic coupling gives rise to 1) four singly accessible redox states with distinct magnetic properties, 2) electron sharing between the two NDI units, and 3) the appearance of a long-lived excimer state with emission in the visible region. Moreover, the extended through-space electron delocalization between the two aromatic faces reduces markedly the first two reduction potentials of the **2NDI**s on account of stabilizing charge resonance effects. In particular, single-electron reduction of the NDI dimer to its radical anion state results in a species having an electronic spectrum indicative of mixed-valence character, while the doubly reduced state is a stabilized radical anion π-dimer at ambient temperatures. In the solid state, the strong intramolecular electronic coupling is accompanied by an enhanced intermolecular electronic coupling, which promotes the formation of almost perfect one-dimensional stacks of **2NDI** cyclophanes.

The two enantiomeric face-to-face (−)- and (+)-**2NDI** cyclophanes were obtained (Figure 1a) from two commercially available building blocks—namely, naphthalenetetracarboxylic dianhydride and either (*RR*)- or (*SS*)-*trans*-1,2-cyclohexanediamine in 10% yield. The absolute configurations of the two enantiomers were confirmed by X-ray diffraction[20] of single crystals obtained by slow vapor diffusion of hexane into 1 mM solutions of (−)- or (+)-**2NDI** in $CHCl_3$. The crystal structures (Figure 1b,c) confirm the rigid geometries of the cyclophane. The two cofacial NDI units in both (−)- or (+)-**2NDI** are separated by an intermolecular distance of 3.5 Å. The ^{1}H NMR spectrum (see Supporting Information, Figure S1) of (−)-2**NDI** revealed only two sets of signals for the eight NDI protons with a downfield shift of 0.6 ppm compared to the monomeric analog, **Ref-NDI**. Such a downfield shift of these signals correlates with the enforced π–π stacking of the aromatic rings. This observation is reinforced by the UV-Vis absorption spectra, which show (Figure 2a) a significant blue-shift of the absorption maximum from 380 nm for **Ref-NDI** to 360 nm for (−)-**2NDI**, indicating exciton coupling in an *H*-aggregate fashion. A weaker yet distinct absorption band ($\lambda \cong 400$ nm) is also observed in the visible spectrum. This unexpected red-shifted electronic transition, which results in these compounds being slightly yellow, both in solution and in the solid state, is most likely a consequence of the small twist angle of 9° between the transition dipole of the two NDI units. This twist renders the formally symmetry-forbidden optical tran-

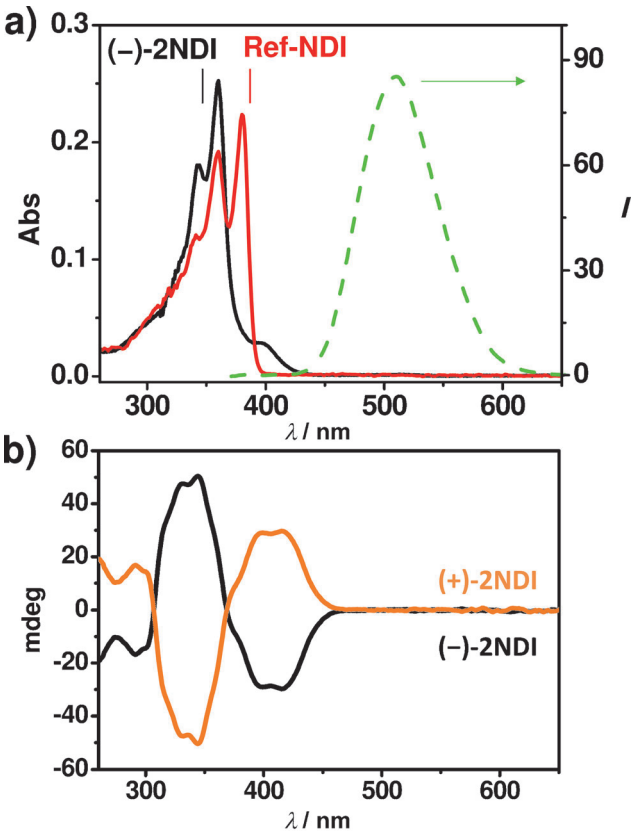

Figure 2. a) UV/Vis Absorption (black trace) and emission (green dotted trace) spectra of (−)-**2NDI** in CH_2Cl_2 compared with the absorption spectra of the **Ref-NDI** (red trace). b) CD Spectra of (−)-**2NDI** (black trace) and (+)-**2NDI** (orange trace) in CH_2Cl_2 at 298 K and a concentration of 10 μM.

sition to the lower energy, exciton-coupled state partially allowed. The chiral environment, induced by the diamine linker and the structural rigidity of the two homochiral (−)- and (+)-**2NDI** cyclophanes, also leads to pronounced chiroptical properties as revealed (Figure 2b) by their circular dichroism (CD) spectra.

(−)-**2NDI** exhibits (Figure 2a) significantly enhanced[21] fluorescence ($\Phi_{fl} = 4.7\,\%$) centered at 515 nm in CH_2Cl_2 solution with 1) a long 20 ns lifetime, 2) a large Stokes shift, and 3) a lack of vibronic features[22] (Figure S5). Pronounced exciton coupling between the two cofacially stacked NDI units is apparent from UV/Vis absorption and CD spectroscopy, demonstrating that the transition dipole moment of one NDI is coupled to that of the second NDI to give rise to excitonic states.[23] Fluorescence spectroscopy reveals that an electron, when photoexcited from the π to π* molecular orbital, is effectively shared between the two NDI units, leading to an emissive excimer-like state, which is an indication of electron delocalization in the π* orbitals.[24]

The cyclic voltammogram (CV) of **Ref-NDI** is characterized (Figure 3a) by two sequential one-electron cathodic waves, observed at −690 mV and −1130 mV vs. Ag/AgCl, corresponding to the formation of the [**Ref-NDI**]$^{\bullet-}$ radical anion and the [**Ref-NDI**]$^{2-}$ dianion, respectively. By contrast, the CV of (−)-**2NDI** features four distinct reversible one-electron waves. The first reduction potential ($E_1 = -365$ mV) is shifted by 325 mV towards more positive potential compared with that ($E_1 = -690$ mV) of **Ref-NDI**, while the second one ($E_2 = -605$ mV) of **2NDI** is shifted by 85 mV. Conversely, the last two reduction potentials (E_3, $E_4 = -1430$, -1665 mV) of **2NDI** are shifted towards more negative potentials compared to the **Ref-NDI**. The fact that splitting of the reduction potentials of **2NDI** occurs at more positive potentials is indicative of electronic communication between the two equivalent NDI redox centers in the cyclophane on account of the mixing of their π-orbitals.

A mixed-valence[25] [**2NDI**]$^{\bullet-}$ species (Figure 3b) can be generated in quantitative yield upon monoreduction of **2NDI** either chemically with 1 equiv of a chemical reductant such as cobaltocene ($CoCp_2$) or electrochemically at −0.5 V, as evidenced (Figure 3c,d) by UV/Vis/NIR and electron paramagnetic resonance (EPR) spectroscopies. Solution phase EPR and electron-nuclear double resonance (ENDOR) studies of the monoreduced radical anion [**2NDI**]$^{\bullet-}$ provide evidence for electron sharing in the radical anion. EPR spectra reveal (Figure 3d) a linewidth of ca. 4 G for [**2NDI**]$^{\bullet-}$ compared with one of 5.7 G observed for [**Ref-NDI**]$^{\bullet-}$.[26] Moreover, the ENDOR spectrum of [**2NDI**]$^{\bullet-}$ reveals (Figure S9) a close to half reduction in the magnitude of the electron-nuclear hyperfine coupling constants (HFCCs) relative to the monomer [**Ref-NDI**]$^{\bullet-}$. These results are consistent with complete sharing of the electron between the two NDI units in the cyclophane radical anion [**2NDI**]$^{\bullet-}$ on the EPR timescale.[27]

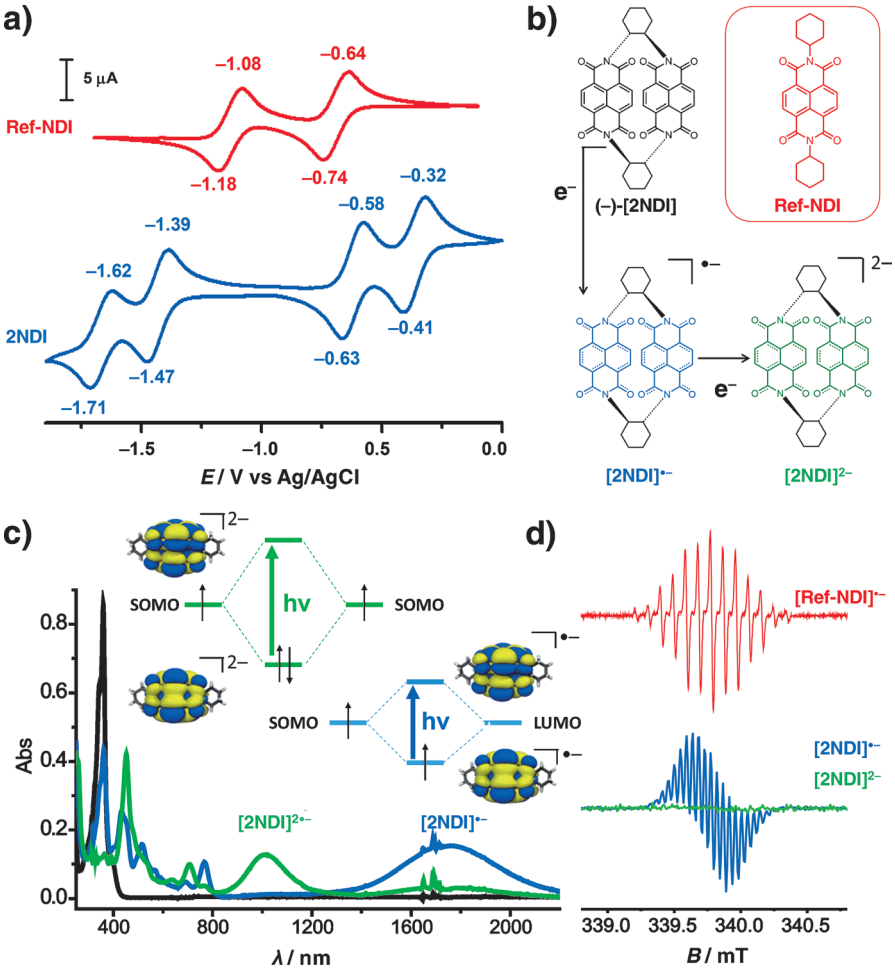

Figure 3. a) Cyclic voltammograms of **Ref-NDI** (red curve) and (−)-**2NDI** (blue curve) recorded (scan rate 50 mV s^{-1}) using a glassy carbon working electrode. All the experiments were performed at 298 K in Ar-purged CH_2Cl_2 solution (0.5 mM) with 0.1 M $[Bu_4N][PF_6]$ as the supporting electrolyte. b) Schematic representation of the distinct reduction steps exhibited by **2NDI**. The two one-electron reductions lead, first of all, to the formation of the mixed-valence dimer [**2NDI**]$^{\bullet-}$, and then to the radical-anion dimer [**2NDI**]$^{2-}$. c) UV/Vis/NIR Absorption spectra of **2NDI** and its reduced states arising from the electrochemical reduction by setting the potentials at −0.5 V (blue trace) and −1.0 V (green trace). The insets show the mixing of the MOs localized on individual NDI units and the lowest energy electronic transitions for [**2NDI**]$^{\bullet-}$ (blue) and [**2NDI**]$^{2-}$ (green). d) EPR Spectra of (−)-**2NDI** after reduction with 1 equiv (blue trace) and 2 equiv (green trace) of $[CoCp_2]$. The EPR spectrum of **Ref-NDI** after reduction with 1 equiv of $[CoCp_2]$ is shown for comparison (red trace). All spectra were recorded in Ar-purged CH_2Cl_2 solution (0.3 mM) at 290 K. The reduction of the EPR-linewidth for (−)-**2NDI** by a factor of $\sqrt{2}$ indicates delocalization of the unpaired electron over both NDI units.

In order to address the degree of unpaired electron delocalization in the **[2NDI]**$^{\bullet-}$ mixed-valence state, measurements were performed (Figure 3c) on the intervalence charge transfer (IVCT) transitions[28] by UV/Vis/NIR spectroelectrochemistry. Changes in absorption were monitored during the electrochemical reduction of **2NDI** at different applied potentials using an optically transparent thin-layer spectroelectrochemical cell. The spectral progression accompanying the one-electron reduction at −0.5 V reveals the appearance of a new band in the NIR region[29] centered at 1750 nm which can be assigned to the IVCT transition. The intensity of this new band decreased as the potential was increased to −1.0 V and another band appeared at around 1000 nm which can be assigned to the doubly reduced **[2NDI]**$^{2-}$—namely, the covalently linked radical anion dimer (Figure 3b) of NDI$^{\bullet-}$ which was also identified (Figure 3d) by the disappearance of the EPR signal as a consequence of strong electron spin pairing within the **[2NDI]**$^{2-}$ cyclophane. No evidence for a ground-state triplet was observed in the CW-EPR spectrum at 77 K. Upon resetting the applied electrical potential to 0.0 V, the neutral dimer was regenerated in > 85 % yield. The IVCT band-shape analysis, based on the Marcus–Hush two-mode model,[28,30] gave the electronic coupling parameters, $\varepsilon_{IVCT} = 1350\,M^{-1}\,cm^{-1}$, $H_{AB} = 1900\,cm^{-1}$. In particular, the experimental bandwidth ($\Delta\nu_{1/2} = 1420\,cm^{-1}$) of IVCT band is narrower than the theoretical one ($\Delta\nu^{\circ}_{1/2} = 3629\,cm^{-1}$ at 298 K) calculated using Hush's theory.[30] This result indicates that **[2NDI]**$^{\bullet-}$ exhibits a high electronic delocalization, typical of Robin–Day Class II–III compounds,[31] in good agreement with the large splitting in the reduction potential revealed by cyclic voltammetry and the change in absorption of **[2NDI]**$^{\bullet-}$ compared to [**Ref-NDI**]$^{\bullet-}$ in the UV/Vis region, an observation which is also indicative of electron delocalization on the fast timescale (10^{14} Hz) of electronic spectroscopy (Figure S4).

The stacking of the **2NDI** molecules in the solid-state superstructure (Figure 4a) imposes a cofacial arrangement upon neighboring cyclophanes in a close-to-ideal alignment of their π-systems. These rigid superstructures provide an optimal arrangement of the NDI molecular orbitals for studying exciton interactions and electron delocalization along their π-systems in the solid state. The packing is characterized by an array of **2NDI** molecules in a slightly slipped π–π stack with the shortest interplanar distance being only 3.25 Å and with close naphthalene-imide [H···O] contacts of 2.4 Å between the arrays of π–π stacks (Figure S3). The considerable π–π overlap in this motif may result in enhanced charge transport properties in the solid state.[8] An unexpected emission, which is detected (Figure 4b) from single crystals of **2NDI**, represents a rare example of photoluminescent single crystals made up entirely of NDI units. The time-resolved photoluminescence of these single crystals shows (Figure 4c) a clear decrease, compared with measurements in solution, of excimer like emission lifetimes in keeping with intermolecular electronic communication in the π–π stacks in the solid state. By contrast, when (−)-**2NDI** is doubly reduced in $CHCl_3$ solution with 2 equiv of $CoCp_2$ in the presence of 2 equiv of Bu_4NPF_6, the resulting single crystals of (−)-**[2NDI]**$^{2-}$·2 Bu_4N^+, on examination (Figure 5)

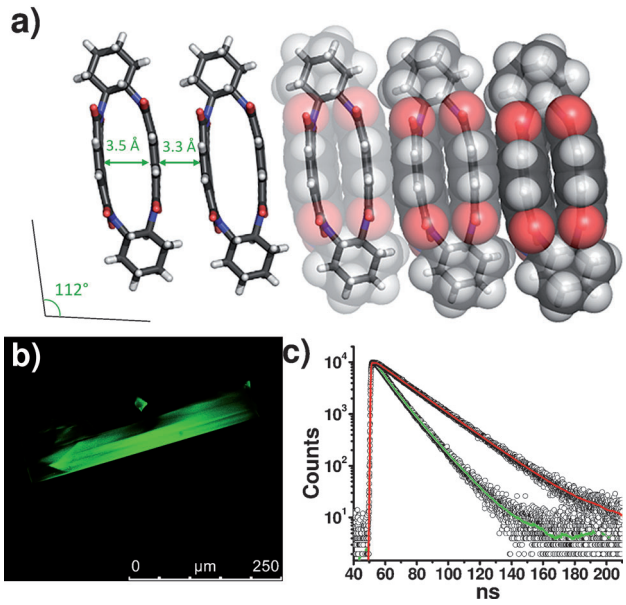

Figure 4. a) A progression from a tubular to a space-filling representation of the solid-state superstructure of (−)-**2NDI**, showing the slightly slipped face-to-face one-dimensional π–π stacks of the NDI units and the intra- and intermolecular distances between them of 3.5 and 3.3 Å, respectively. b) A fluorescence microscope image of a representative single crystal of (−)-**2NDI**, illuminated with a diode laser at 405 nm. c) The decays in photoluminescence of (−)-**2NDI** in CH_2Cl_2 solution (10 µM) (red trace) and in a single crystal (green trace), showing the decrease in excimer-like emission lifetimes on going from solution to the solid state.

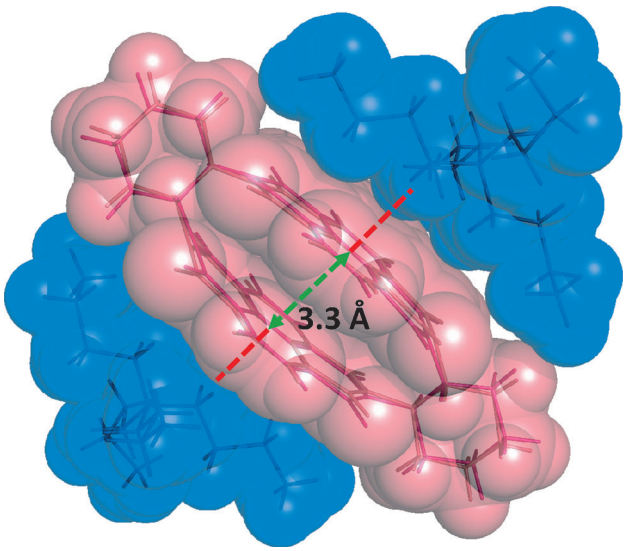

Figure 5. A space-filling representation of the solid-state superstructure of [(−)-**2NDI**]$^{2-}$·2 Bu_4N^+ in which the radical anion dimer is illustrated in pink while the two tetrabutylammonium ions are illustrated in blue. A tubular representation (pale pink and dark blue) of the same solid-state structure, which shows the intramolecular π–π stacking distance between the two NDI$^{\bullet-}$ radical anions, is superimposed upon the space-filling representation. Note that there are [C–H···π] interactions between the NDI$^{\bullet-}$ radical anions and the Bu_4N^+ cations. The calculated structure (dark pink tubular skeleton) of [(−)-**2NDI**]$^{2-}$ is overlaid with the solid-state structure of the cyclophane for comparison.

produce a discrete superstructure[20] devoid of intermolecular π–π stacking interactions. In the case of (−)-**[2NDI]$^{2-}$**·2 Bu_4N^+, intermolecular interactions between the radical anion dimer and the tetrabutylammonium ions disrupt further π–π stacking interactions beyond the molecule. Analysis of the solid-state structure of (−)-**[2NDI]$^{2-}$** demonstrates that its two NDI units are drawn closer together (3.3 Å) and orient themselves more closely in register, as indicated by the decrease in the twist angle between them from 9.0° to 7.5°. This observation indicates that a stabilizing interaction must be present from the electron delocalization and spin-pairing of NDI radical anions, an interaction that prevails over the Coulombic repulsion arising from their dimerization.[32]

We have demonstrated efficient π-orbital overlap leading to complete through-space electron delocalization between two rigid cofacial NDI units, covalently linked within a rigid cyclophane scaffold. Cyclic voltammetry reveals that the enforced electronic interaction leads to four individually accessible redox states, which can be isolated and characterized in solution and in the solid state. The neutral state is strongly exciton coupled and has sufficient electronic coupling between the π-systems to produce a long-lived emissive excited state indicative of extensive electron delocalization between the two NDI units. The solid-state superstructure found in the single crystal shows a nearly perfect alignment of the NDI moieties, indicating strong intermolecular π-orbital overlap. The monoreduced radical anion **[2NDI]$^{\bullet-}$**, which is paramagnetic, is a mixed-valence species. The Gaussian-shaped absorption band centered at 1750 nm for this radical anion state has been used to calculate the electronic coupling matrix element H_{AB} by applying Marcus-Hush theory. Lineshape analysis points to a highly delocalized class II–III system, in agreement with experimental evidence. On the other hand, the radical anion dimer (−)-**[2NDI]$^{2-}$** is diamagnetic. The crystal structure of this radical anion dimer confirms and highlights, with crystallographic precision, extensive π-electron delocalization interaction between two NDI$^{\bullet-}$ radical anions upon spin-pairing. The fundamental understanding and distinction, at the molecular level, of the subtle balance between the through-space charge resonance interaction in the radical-neutral mixed-valence π-stacks and the competitive diamagnetic radical-dimerization of the π-stacks, is essential for the development of more efficient organic electronic devices.[33]

Received: March 29, 2014
Published online: July 10, 2014

Keywords: cyclophane · excimer emission · mixed-valence compounds · radical anion dimer · π-electron delocalization

[1] a) C. A. Hunter, J. K. M. Sanders, *J. Am. Chem. Soc.* **1990**, *112*, 5525 – 5534; b) E. A. Meyer, R. K. Castellano, F. Diederich, *Angew. Chem.* **2003**, *115*, 1244 – 1287; *Angew. Chem. Int. Ed.* **2003**, *42*, 1210 – 1250; c) A. P. H. J. Schenning, E. W. Meijer, *Chem. Commun.* **2005**, 3245 – 3258.

[2] a) R. Bhosale, J. Misek, N. Sakai, S. Matile, *Chem. Soc. Rev.* **2010**, *39*, 138 – 149; b) S. Sengupta, F. Würthner, *Acc. Chem. Res.* **2013**, *46*, 2498 – 2512.

[3] a) H. E. Katz, A. J. Lovinger, J. Johnson, C. Kloc, T. Siegrist, W. Li, Y. Y. Lin, A. Dodabalapur, *Nature* **2000**, *404*, 478 – 481; b) M. Muccini, *Nat. Mater.* **2006**, *5*, 605 – 613; c) A. Saeki, Y. Koizumi, T. Aida, S. Seki, *Acc. Chem. Res.* **2012**, *45*, 1193 – 1202.

[4] C. L. Wang, H. L. Dong, W. P. Hu, Y. Q. Liu, D. B. Zhu, *Chem. Rev.* **2012**, *112*, 2208 – 2267.

[5] J. L. Bredas, J. P. Calbert, D. A. da Silva, J. Cornil, *Proc. Natl. Acad. Sci. USA* **2002**, *99*, 5804 – 5809.

[6] M. Mas-Torrent, C. Rovira, *Chem. Rev.* **2011**, *111*, 4833 – 4856.

[7] a) V. C. Sundar, J. Zaumseil, V. Podzorov, E. Menard, R. L. Willett, T. Someya, M. E. Gershenson, J. A. Rogers, *Science* **2004**, *303*, 1644 – 1646; b) T. He, M. Stolte, F. Würthner, *Adv. Mater.* **2013**, *25*, 6951 – 6955; c) F. G. Brunetti, C. Romero-Nieto, J. López-Andarias, C. Atienza, J. L. López, D. M. Guldi, N. Martín, *Angew. Chem.* **2013**, *125*, 2236 – 2240; *Angew. Chem. Int. Ed.* **2013**, *52*, 2180 – 2184.

[8] a) H. Najafov, B. Lee, Q. Zhou, L. C. Feldman, V. Podzorov, *Nat. Mater.* **2010**, *9*, 938 – 943; b) V. Podzorov, *Nat. Mater.* **2010**, *9*, 616 – 617; c) T. Aida, E. W. Meijer, S. I. Stupp, *Science* **2012**, *335*, 813 – 817.

[9] a) S. Grimme, *Angew. Chem.* **2008**, *120*, 3478 – 3483; *Angew. Chem. Int. Ed.* **2008**, *47*, 3430 – 3434; b) M. Gallego, J. Calbo, J. Aragó, R. M. Krick Calderon, F. H. Liquido, T. Iwamoto, A. K. Greene, E. A. Jackson, E. M. Pérez, E. Ortí, D. M. Guldi, L. T. Scott, N. Martín, *Angew. Chem.* **2014**, *126*, 2035 – 2040; *Angew. Chem. Int. Ed.* **2014**, *53*, 2170 – 2175.

[10] a) S. V. Bhosale, C. H. Jani, S. J. Langford, *Chem. Soc. Rev.* **2008**, *37*, 331 – 342; b) H. Yan, Z. Chen, Y. Zheng, C. Newman, J. R. Quinn, F. Dötz, M. Kastler, A. Facchetti, *Nature* **2009**, *457*, 679 – 686.

[11] a) P. Mukhopadhyay, Y. Iwashita, M. Shirakawa, S. Kawano, N. Fujita, S. Shinkai, *Angew. Chem.* **2006**, *118*, 1622 – 1625; *Angew. Chem. Int. Ed.* **2006**, *45*, 1592 – 1595; b) N. Ponnuswamy, G. D. Pantos, M. M. J. Smulders, J. K. M. Sanders, *J. Am. Chem. Soc.* **2012**, *134*, 566 – 573; c) G. Sforazzini, E. Orentas, A. Bolag, N. Sakai, S. Matile, *J. Am. Chem. Soc.* **2013**, *135*, 12082 – 12090.

[12] a) N. Sakai, R. Bhosale, D. Emery, J. Mareda, S. Matile, *J. Am. Chem. Soc.* **2010**, *132*, 6923 – 6925; b) X. W. Zhan, A. Facchetti, S. Barlow, T. J. Marks, M. A. Ratner, M. R. Wasielewski, S. R. Marder, *Adv. Mater.* **2011**, *23*, 268 – 284.

[13] a) J. Míšek, A. V. Jentzsch, S. I. Sakurai, D. Emery, J. Mareda, S. Matile, *Angew. Chem.* **2010**, *122*, 7846 – 7849; *Angew. Chem. Int. Ed.* **2010**, *49*, 7680 – 7683; b) L. E. Santos-Figueroa, M. E. Moragues, E. Climent, A. Agostini, R. Martínez-Máñez, F. Sancenón, *Chem. Soc. Rev.* **2013**, *42*, 3489 – 3613.

[14] a) R. E. Dawson, A. Hennig, D. P. Weimann, D. Emery, V. Ravikumar, J. Montenegro, T. Takeuchi, S. Gabutti, M. Mayor, J. Mareda, C. A. Schalley, S. Matile, *Nat. Chem.* **2010**, *2*, 533 – 538; b) A. V. Jentzsch, A. Hennig, J. Mareda, S. Matile, *Acc. Chem. Res.* **2013**, *46*, 2791 – 2800.

[15] Y. J. Zhao, Y. Domoto, E. Orentas, C. Beuchat, D. Emery, J. Mareda, N. Sakai, S. Matile, *Angew. Chem.* **2013**, *125*, 10124 – 10127; *Angew. Chem. Int. Ed.* **2013**, *52*, 9940 – 9943.

[16] a) N. Ponnuswamy, F. B. L. Cougnon, J. M. Clough, G. D. Pantos, J. K. M. Sanders, *Science* **2012**, *338*, 783 – 785; b) C. J. Bruns, J. Li, M. Frasconi, S. T. Schneebeli, J. Iehl, H. P. Jacquot de Rouville, S. I. Stupp, G. A. Voth, J. F. Stoddart, *Angew. Chem.* **2014**, *126*, 1984 – 1989; *Angew. Chem. Int. Ed.* **2014**, *53*, 1953 – 1958.

[17] a) J. Jazwinski, A. J. Blacker, J.-M. Lehn, M. Cesario, J. Guilhem, C. Pascard, *Tetrahedron Lett.* **1987**, *28*, 6057 – 6060; b) A. Takai, T. Yasuda, T. Ishizuka, T. Kojima, M. Takeuchi, *Angew. Chem.* **2013**, *125*, 9337 – 9341; *Angew. Chem. Int. Ed.* **2013**, *52*, 9167 – 9171.

[18] a) S. Gabutti, M. Knutzen, M. Neuburger, G. Schull, R. Berndt, M. Mayor, *Chem. Commun.* **2008**, 2370 – 2372; b) F. Matino, G. Schull, F. Köhler, S. Gabutti, M. Mayor, R. Berndt, *Proc. Natl. Acad. Sci. USA* **2011**, *108*, 961 – 964.

[19] P. Delhaes, *Graphite and Precursors*, Gordon & Breach, Marston, Amsterdam Abingdon, **2001**.

[20] Crystal data for (−)-**2NDI**: $[C_{40}H_{28}N_4O_8]$. MW = 692.66, triclinic, space group $P\bar{1}$ (no. 1), $a = 7.0255(5)$, $b = 14.6532(11)$, $c = 22.0962(17)$ Å, $\alpha = 86.353(3)$, $\beta = 87.271(3)$, $\gamma = 80.237(2)°$, $V = 2235.7(3)$ Å^3, $Z = 3$, $T = 100(2)$ K, μ(Cu-Kα) = 0.904 mm^{-1}, $\rho_{calc} = 1.543$ g m^{-1} m^3, 19788 reflections measured ($6.13 \le 2\theta \le 130.494$), 14052 unique, which were used in all calculations. The final R_1 was 0.0405 ($I > 2\sigma(I)$) and wR_2 was 0.1082 (all data). Crystal data for (+)-**2NDI**: $[C_{40}H_{28}N_4O_8]\cdot(CHCl_3)$. MW = 818.03, orthorhombic, space group $P2_12_12_1$ (no. 19), $a = 6.9206(15)$, $b = 33.914(7)$, $c = 43.889(9)$ Å, $V = 10301(4)$ Å^3, $Z = 12$, $T = 100.01$ K, μ(Cu-Kα) = 2.976 mm^{-1}, $\rho_{calc} = 1.571$ g m^{-1} m^3, 10182 reflections measured ($3.292 \le 2\theta \le 101.394$), 10160 unique, which were used in all calculations. The final R_1 was 0.0877 ($I > 2\sigma(I)$) and wR_2 was 0.2188 (all data). Crystal data for $[(-)\text{-}\mathbf{2NDI}]^{2-}\cdot 2\,Bu_4N^+$): $[C_{72}H_{100}N_4O_8]\cdot(CHCl_3)_4$. MW = 1655.05, monoclinic, space group $P2_1$, $a = 15.6525(9)$, $15.1587(9)$, $c = 18.3802(14)$ Å, $\alpha = 90$, $\beta = 114.498(2)$, $\gamma = 90°$, $V = 3968.5(4)$ Å^3, $Z = 2$, $T = 100(2)$ K, μ(Cu-Kα) = 4.296 mm^{-1}, $\rho_{calc} = 1.385$ g cm^{-3}, 51585 reflections measured ($5.284 \le 2\theta \le 136.618$), 14216 unique, which were used in all calculations. The final R_1 was 0.0817 ($I > 2\sigma(I)$) and wR_2 was 0.2371 (all data). CCDC 994126 ((−)-**2NDI**), 994127 ((+)-**2NDI**), and 994128 ($[(-)\text{-}\mathbf{2NDI}]^{2-}\cdot 2\,Bu_4N^+$) contain the supplementary crystallographic data for this paper. These data can be obtained free of charge from The Cambridge Crystallographic Data Centre via www.ccdc.cam.ac.uk/data_request/cif.

[21] The fluorescence of **Ref-NDI** in solution is barely detectable ($\lambda_{em} = 385$ nm, $\Phi_{fl} < 10^{-5}$) as a result of extremely fast and efficient intersystem crossing from the excited singlet state to a lower triplet state. See: P. Ganesan, J. Baggerman, H. Zhang, E. J. R. Sudholter, H. Zuilhof, *J. Phys. Chem. A* **2007**, *111*, 6151 – 6156.

[22] This excimer-like emission has only been observed previously for self-assembled π-stacks of NDI units in either H_2O or PhMe, and has been used to monitor the aggregation of NDI chromophores. Unlike these dynamic supramolecular systems, which display complex multiexponential decay kinetics on account of multiple populations, the covalently assembled **2NDI** exhibits (Figure S5b) a monoexponential decay in keeping with its discrete dimeric nature. The intrinsic rigidity of the cyclophane limits the relaxation from the excimer-like state to the ground state, accounting for its extended excited-state lifetime. For a more detailed discussion, see: a) H. N. Lee, Z. C. Xu, S. K. Kim, K. M. K. Swamy, Y. Kim, S. J. Kim, J. Yoon, *J. Am. Chem. Soc.* **2007**, *129*, 3828 – 3829; b) S. Basak, J. Nanda, A. Banerjee, *Chem. Commun.* **2013**, *49*, 6891 – 6829; c) R. F. Fink, J. Seibt, V. Engel, M. Renz, M. Kaupp, S. Lochbrunner, H. M. Zhao, J. Pfister, F. Würthner, B. Engels, *J. Am. Chem. Soc.* **2008**, *130*, 12858 – 12859.

[23] It is important to remember that the observed exciton coupling does not mean that there is any electron exchange between the NDI units, but rather that the excitation energy is being shared between them. See: M. Kasha, H. R. Rawles, M. L. El-Bayoumi, *Pure Appl. Chem.* **1965**, *11*, 371 – 392.

[24] The delocalization hypothesis is supported by density functional theory (DFT) calculations performed at the M06-2X/6-31G** level of theory, which gives rise to delocalized frontier molecular orbitals (Figure 3c) in (−)-**2NDI**.

[25] a) S. F. Nelsen, *Chem. Eur. J.* **2000**, *6*, 581 – 588; b) K. D. Demadis, C. M. Hartshorn, T. J. Meyer, *Chem. Rev.* **2001**, *101*, 2655 – 2686; c) B. S. Brunschwig, C. Creutz, N. Sutin, *Chem. Soc. Rev.* **2002**, *31*, 168 – 184; d) A. Heckmann, C. Lambert, *Angew. Chem.* **2012**, *124*, 334 – 404; *Angew. Chem. Int. Ed.* **2012**, *51*, 326 – 392.

[26] According to the Norris relationship, this observation corresponds to a decrease in linewidth of a factor of $\sqrt{2}$, a situation which is consistent with complete electron delocalization over both NDI units in $[\mathbf{2NDI}]^{\bullet-}$ on the CW-EPR timescale (10^7 Hz). See: J. R. Norris, R. A. Uphaus, H. L. Crespi, J. Katz, *Proc. Natl. Acad. Sci. USA* **1971**, *68*, 625 – 628.

[27] a) M. J. Tauber, R. F. Kelley, J. M. Giaimo, B. Rybtchinski, M. R. Wasielewski, *J. Am. Chem. Soc.* **2006**, *128*, 1782 – 1783; b) T. M. Wilson, M. J. Tauber, M. R. Wasielewski, *J. Am. Chem. Soc.* **2009**, *131*, 8952 – 8957; c) T. M. Wilson, T. A. Zeidan, M. Hariharan, F. D. Lewis, M. R. Wasielewski, *Angew. Chem.* **2010**, *122*, 2435 – 2438; *Angew. Chem. Int. Ed.* **2010**, *49*, 2385 – 2388; d) S. T. Schneebeli, M. Frasconi, Z. Liu, L. Wu, D. M. Gardner, N. L. Strutt, C. Y. Cheng, R. Carmieli, M. R. Wasielewski, J. F. Stoddart, *Angew. Chem.* **2013**, *125*, 13338 – 13342; *Angew. Chem. Int. Ed.* **2013**, *52*, 13100 – 13104.

[28] The examination of the IVCT band shape based on Marcus – Hush theory is generally considered to be a more accurate probe of the extent of charge delocalization. For more details, see Ref. [25] and N. S. Hush, *Prog. Inorg. Chem.* **1967**, *8*, 391 – 444.

[29] The monomeric **Ref-NDI** and its monoreduced radical anion $[\mathbf{Ref\text{-}NDI}]^{\bullet-}$ do not absorb in the NIR region because of the extremely low association constant for the radical anion dimerization. See: a) V. Ganesan, S. V. Rosokha, J. K. Kochi, *J. Am. Chem. Soc.* **2003**, *125*, 2559 – 2571; b) J. M. Spruell, *Pure Appl. Chem.* **2010**, *82*, 2281 – 2294.

[30] The theoretical IVCT bandwidth ($\Delta\nu°_{1/2} = (2.310(\nu_{max}))^{1/2}$ at 298 K) was calculated on the basis of Hush's classical two-state theory. See: B. Bechlars, D. M. D'Alessandro, D. M. Jenkins, A. T. Iavarone, S. D. Glover, C. P. Kubiak, J. R. Long, *Nat. Chem.* **2010**, *2*, 362 – 368.

[31] P. Day, N. S. Hush, R. J. Clark, *Philos. Trans. R. Soc. London Ser. A* **2008**, *366*, 5 – 14.

[32] Attempts to grow single crystals of the mixed-valence state have resulted so far in long red needles that are too thin for us to be able to collect X-ray diffraction data. We are currently working on the optimization of the crystallization conditions in order to obtain larger crystals. Neverthless, the preferential one-dimentional crystal growth suggests strong intermolecular π–π stacking interactions between the cyclophanes as a result of electron delocalizaion.

[33] a) L. L. Miller, K. R. Mann, *Acc. Chem. Res.* **1996**, *29*, 417 – 423; b) A. S. Jalilov, S. F. Nelsen, I. A. Guzei, Q. Wu, *Angew. Chem.* **2011**, *123*, 6992 – 6995; *Angew. Chem. Int. Ed.* **2011**, *50*, 6860 – 6863.

